Assessment of the Thermodynamic Stability of Thermal Insulating Materials in Aluminium Electrolysis Cells

Raymond Luneng[1], Tor Grande[2] and Arne Petter Ratvik[3]
1. PhD-candidate
2. Professor
Department of Materials Science and Engineering, Norwegian University of Science and Engineering (NTNU), Trondheim, Norway.
3. Senior Research Scientist, SINTEF Materials and Chemistry, Trondheim, Norway.
Corresponding author: raymond.luneng@ntnu.no

Abstract

The cathode bottom lining in aluminium electrolysis cells serves as a thermal insulating barrier and is important for the overall thermal and dimensional stability of the cell. The thermal insulation layer is protected against chemical degradation by a refractory layer, but due to recent technological developments and new cell designs, the stability of insulating materials is expected to become an important matter of concern in the years to come. The thermodynamic stability of thermal insulating materials in chemical environment corresponding to the one below the carbon cathode has been assessed. Thermodynamic evaluation was used to predict possible chemical reactions caused by sodium vapour, which possibly can penetrate through the refractory barrier and react with the insulation material. The most likely chemical reactions with the insulation materials were identified by minimization of Gibbs energy of the system. Changes in the mineralogical composition of the insulation materials were predicted based on the thermodynamic calculations. The structural integrity of the thermal insulation materials is discussed in relation to the mineralogical changes predicted based on the thermodynamic assessment.

Keywords: Thermal insulating materials; aluminium electrolysis cell; thermodynamic stability; degradation.

1. Introduction

The process of producing aluminium by molten salt electrolysis is energy demanding, and a considerable amount of the energy input is lost in the form of heat release to the surroundings [1]. The electrolysis cells are designed with sidewalls of materials having high thermal conductivity in order to form a frozen layer of bath, the sideledge, which will protect the sidelining and potshell from the corrosive nature of the bath. The bottom of the cell is designed in such a way to minimize energy loss by using a layer of materials with low thermal conductivity in the bottom lining, below the refractory layer [2]. The thermal insulation layer will also reduce possible solidification of the bath towards the cathode [1]. The most typical thermal insulating materials used in this layer are moler (diatomite), calcium silicate, or vermiculite based materials [2]. The thermal insulating layer is critical for the overall thermal and dimensional stability of the cell [1, 2]. A layer of refractory materials is placed above the insulating layer in order to protect it from bath components or volatile species that may penetrate through the carbon cathode blocks [2].

At present, the cell lifetime is in most cases limited by the carbon cathode wear [3]. The cathode wear and reduced lifetime of the cells have become a major challenge as the industry have progressed towards high amperage cells [3, 4]. Increased lifetime of the cells can be achieved by increasing the carbon cathode thickness on the expense of the refractory layer. This will put higher demand on the thermal insulating layer, and may increase the exposure to gas species

such as Na and $NaAlF_4$, which can react with the highly porous insulation material with dramatic changes in the thermal conductivity and the thermal profile of the cell and, consequently, the energy loss. The stability of the thermal insulation materials have not received much attention in the literature [5, 6], but the forecast to reduce the thickness of the refractory layer actuates the understanding of the chemical and thermal stability. In addition, the shift towards lean cells (low energy cells) will require better insulated cells, as less heat is generated to maintain operational temperature. Evidently, in this case, the heat gradient will increase towards the insulation.

Sodium vapour is most likely [7, 8] the first chemical species diffusing through the refractory layer. Mineralogical changes in the materials due to reaction with sodium are investigated by computational thermodynamics for diatomite, calcium silicate and vermiculite based materials. The findings are discussed with respect to the chemical stability and structural integrity of the thermal insulation layer in the electrolysis cells.

2. Method

The thermodynamic assessment of the different insulation materials was carried out by use of equilibrium calculations, through minimization of Gibb's energy, in the thermochemical software FactSage™ (version 7.0). This software contains various modules and databases and allows the user to do various equilibrium calculations [9]. In this work, the *Equilibrium* module has been used in combination with the *FactPS* database to analyse the phase composition of the insulation materials during increasing amounts of sodium vapour. The weight percent chemical composition of calcium silicate, vermiculite, and moler materials investigated are presented in Table 1. A simplified composition of each material, where any oxide below 4 wt% has been disregarded, has also been analysed and is listed with a superscript "a" in the same table. Including the loss on ignition (LOI), the mass sums up to approximately 100 wt% for the full composition of all three materials, and a little less for the simplified compositions. This was used as input in the software, i.e. the simplified compositions have slightly less starting mass than the full compositions. The calculations were performed at a temperature of 970 °C, which is higher than the more common 850 °C isotherm in today's operating cells. However, with decreasing thickness of the refractory layer the insulation layer isotherm is bound to increase. Additionally, all main phases were the same at 850 °C. Solid phases with amount less than 1 wt% are not shown in the figures.

Table 1. Chemical composition of the different insulation materials investigated.

Product	SiO_2	Al_2O_3	Fe_2O_3	MgO	CaO	Na_2O	K_2O	SO_3	LOI*
Calcium silicate	47	0.3	0.3	0.6	45	0.1	0.1	N/A	6
Calcium silicate[a]	47	0	0	0	45	0	0	N/A	N/A
Vermiculite	47	7	4	21	2	0.5	11	N/A	7
Vermiculite[a]	47	7	0	21	0	0	11	N/A	N/A
Moler	77	9	7	1.3	0.8	0.6	1.5	1.2	1.5
Moler[a]	77	9	7	0	0	0	0	0	N/A

LOI*: Loss on ignition given at 1025 °C.
[a]: Simplified composition, i.e. any oxide below 4 wt% is disregarded in the calculation.

3. Results

3.1. Calcium silicate materials

Calcium silicate is mainly silica and lime, with only small fractions of other oxide impurities. The content of other phases in calcium silicate is therefore minor and does not influence

significantly the calculated phase content (less than 1 wt%). The amount of the different phases as function of increased sodium vapour exposure can be seen in Figure 1. Additionally, the composition region of the main reactions taking place are marked with blue numbers on the x-axis.

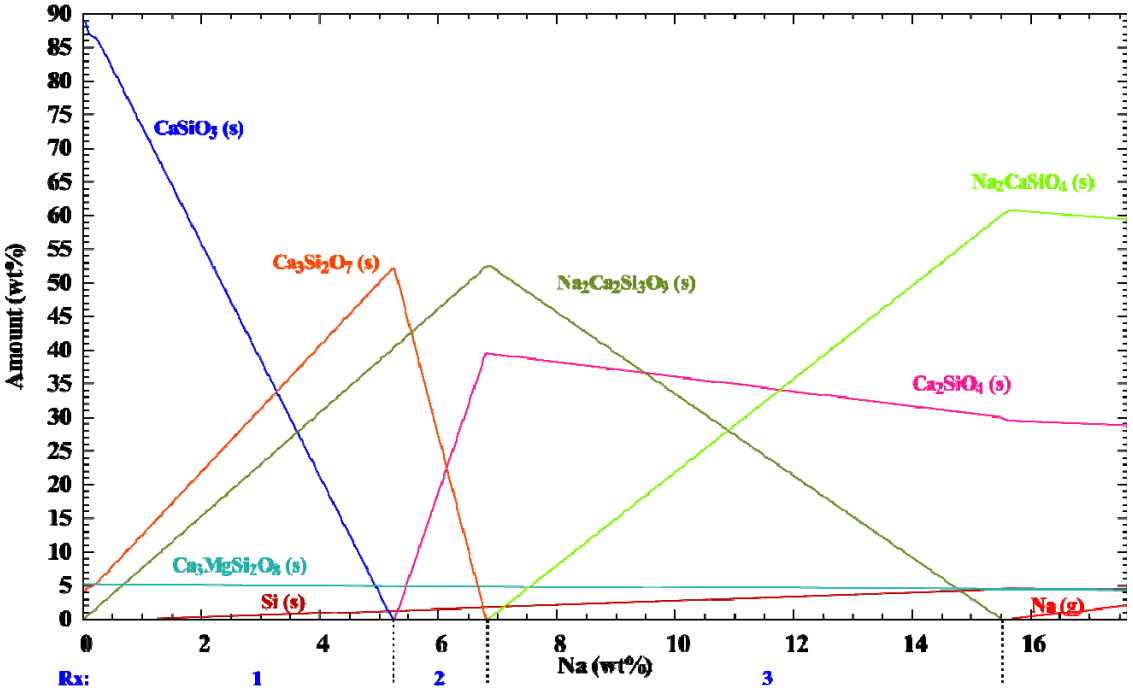

Figure 1: Exposure of calcium silicate to sodium vapour. No further reaction takes place after addition of approximately 15.5 wt% sodium. The blue numbers on the x-axis mark the different chemical reactions taking place, specified in Equations (1) – (3).

The first reaction taking place when calcium silicate is exposed to sodium vapour is reduction of silicon in the wollastonite, $CaSiO_3$(s), phase forming elemental Si(s). Rankinite, $Ca_3Si_2O_7$(s), and combeite, $Na_2Ca_2Si_3O_9$(s), are the additional silicate products formed by the initial reaction. The balanced reaction is given in Equation (1) below.

$$13CaSiO_3 + 4Na = 3Ca_3Si_2O_7 + 2Na_2Ca_2Si_3O_9 + Si \quad (1)$$

Wollastonite is completely consumed by Reaction (1) by only about 5 wt% addition of sodium.

The next major reaction is the continued reduction of silicon in silicate phases at the expense of the rankinite phase, where combeite and calcium orthosilicate, Ca_2SiO_4(s), are the additional products, which continues to about 7 wt% of sodium vapour. The balanced reaction is given below in Equation (2).

$$10Ca_3Si_2O_7 + 4Na = 13Ca_2SiO_4 + 2Na_2Ca_2Si_3O_9 + Si \quad (2)$$

The final major reaction taking place is given in Equation (3). Here, combeite and calcium orthosilicate react with the sodium vapour and form silicon and a sodium calcium orthosilicate, Na_2CaSiO_4(s).

$$Ca_2SiO_4 + 4Na_2Ca_2Si_3O_9 + 12Na = 10Na_2CaSiO_4 + 3Si \quad (3)$$

After the addition of about 15.5 wt% of sodium, no further reaction with the material takes place and the two remaining orthosilicates are stable in and coexistent with metallic sodium.

The minor reduction in the Ca_2SiO_4 content right before Na-saturation is due to the following minor reaction:

$$12Ca_2SiO_4 + 28Na + 16NaAlSiO_4 = 21Na_2CaSiO_4 + Na_2Ca_3Al_{16}O_{28} + 7Si \qquad (4)$$

3.2. Vermiculite materials

The simplified composition of vermiculite materials given in Table 1 largely accounts for all the major phases present in the pristine material and the major phases formed during exposure. The phase composition due to Na exposure is shown in Figure 2. As the simplified composition takes into account most of the major phases, the reactions taking place with increasing amount of sodium vapour consumed are given in Table 2.

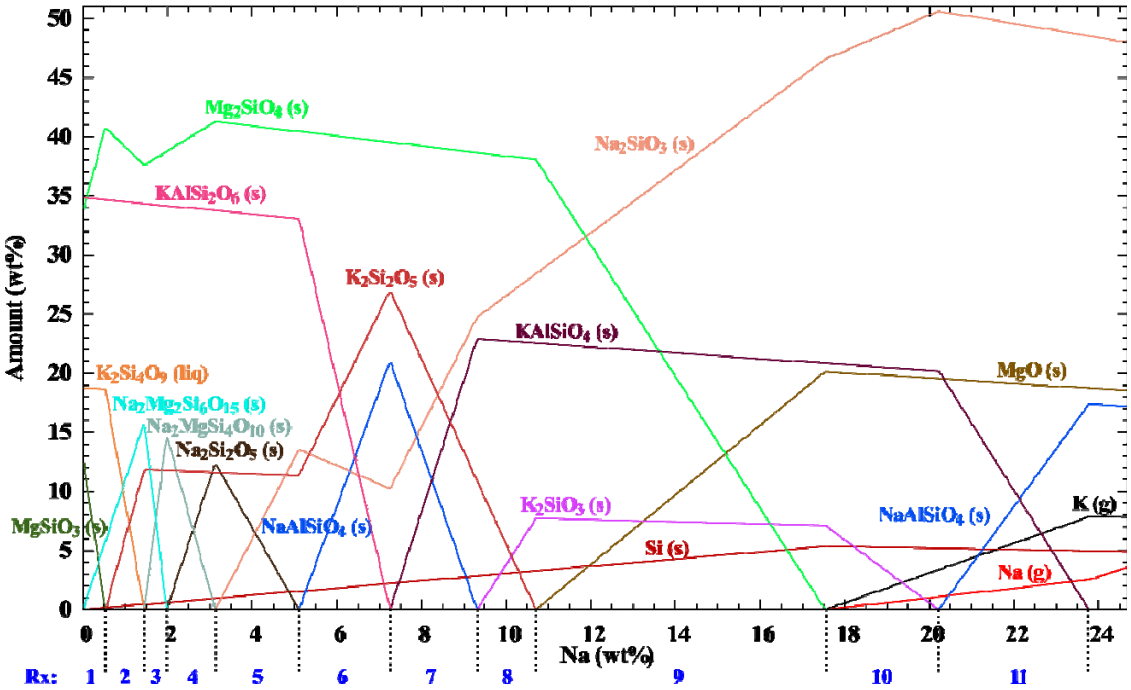

Figure 2. Exposure of the simplified vermiculite composition to sodium vapour. The blue numbers on the x-axis mark the different chemical reactions taking place, specified in Table 2. Na saturation at 24 wt%.

Table 2. Chemical reactions for the simplified vermiculite composition when exposed to sodium vapour. The reaction number corresponds to the numbers given in Figure 2.

Reaction number	Chemical reaction
1	$22MgSiO_3 + 4Na = 9Mg_2SiO_4 + 2Na_2Mg_2Si_6O_{15} + Si$
2	$4Mg_2SiO_4 + 11K_2Si_4O_9 + 8Na = 11K_2Si_2O_5 + 4Na_2Mg_2Si_6O_{15} + 2Si$
3	$16Na_2Mg_2Si_6O_{15} + 12Na = 5Mg_2SiO_4 + 22Na_2MgSi_4O_{10} + 3Si$
4	$10Na_2MgSi_4O_{10} + 12Na = 5Mg_2SiO_4 + 16Na_2Si_2O_5 + 3Si$
5	$3Na_2Si_2O_5 + 4Na = 5Na_2SiO_3 + Si$
6	$Na_2SiO_3 + 6KAlSi_2O_6 + 4Na = 6NaAlSiO_4 + 3K_2Si_2O_5 + Si$
7	$6NaAlSiO_4 + 3K_2Si_2O_5 + 4Na = 5Na_2SiO_3 + 6KAlSiO_4 + Si$
8	$3K_2Si_2O_5 + 4Na = 2Na_2SiO_3 + 3K_2SiO_3 + Si$
9	$3Mg_2SiO_4 + 4Na = 2Na_2SiO_3 + 6MgO + Si$
10	$K_2SiO_3 + 2Na = Na_2SiO_3 + 2K$
11	$KAlSiO_4 + Na = NaAlSiO_4 + K$

The presence of iron oxide in the vermiculite materials is relevant for the reactions taking place at the initial stage of sodium exposure, see Figure 3, which delays the reduction of silicon in the silicate phases. A stable iron phase, Fe_3Si_7(s), is present after sodium vapour saturation, which occurs at about 22.5 wt%. In addition, $Na_4CaSi_3O_9$(s) is formed early in the actual composition of vermiculite and the phase remains stable throughout the exposure.

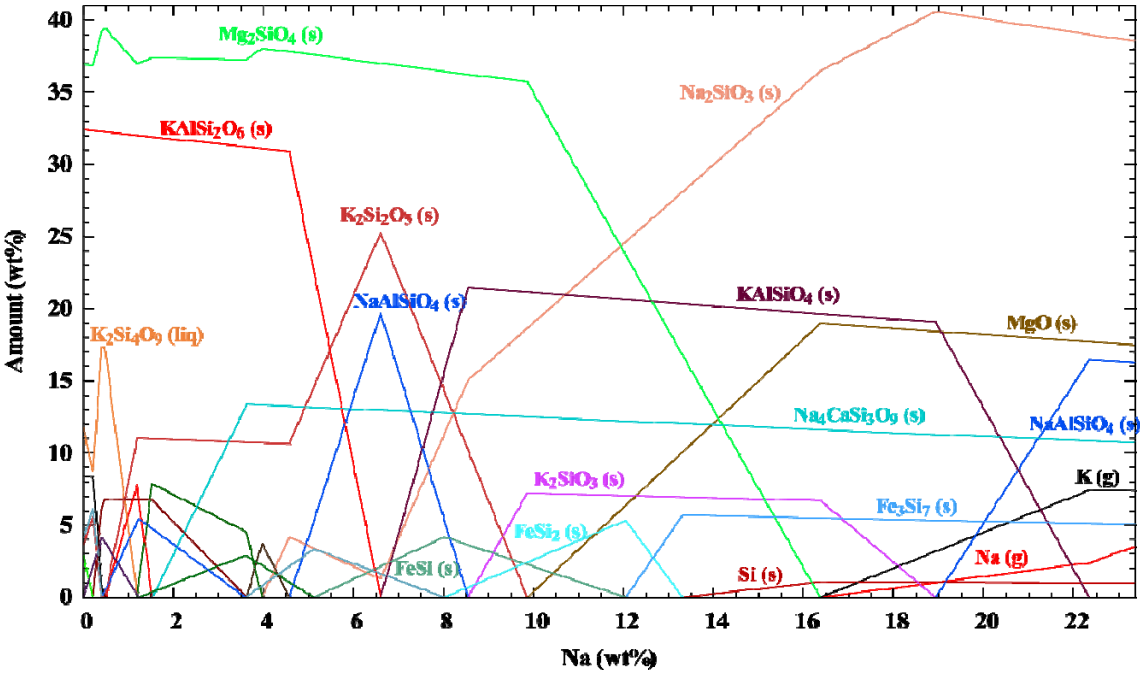

Figure 3. Exposure of the vermiculite composition to sodium vapour. No further reaction takes place after addition of approximately 22.5 wt% sodium.

There are several minor phases formed during the first 4 wt% of sodium vapour, and the phase content in this region is provided in Figure 4. Notice that the major phase Mg_2SiO_4(s) phase is not included in the figure, while the content of $K_2Si_4O_9$(liq) is rapidly increasing and declining in the initial stage. The reactions taking place during the first 4 wt% of sodium exposure of the vermiculite composition are given in Table 3.

Table 3. Chemical reactions for the vermiculite composition when exposed to up to 4 wt% sodium vapour. See Figure 4 for reference to phase compositions.

Na (wt%)	Chemical reaction
0-0.21	$K_2Si_4O_9 + 2Fe_2O_3 + Na = NaFeSi_2O_6 + K_2Si_2O_5 + Fe_3O_4$
0.21-0.42	$4CaMgSi_2O_6 + 3NaFeSi_2O_6 + 3K_2Si_2O_5 + Na = 3K_2Si_4O_9 + 2Na_2Ca_2Si_3O_9 + 2Mg_2SiO_4 + Fe_3O_4$
0.48-1.21	$4Mg_2SiO_4 + 13K_2Si_4O_9 + 4Fe_3O_4 + 8Na = 4Na_2Mg_2Si_6O_{15} + 13K_2Si_2O_5 + 6Fe_2SiO_4$
1.23-1.53	$4Na_2Mg_2Si_6O_{15} + Fe_2SiO_4 + 4Na = 6Na_2MgSi_4O_{10} + Mg_2SiO_4 + 2Fe$
1.53-3.62	$2Na_2MgSi_4O_{10} + 4Na_2Ca_2Si_3O_9 + 5Fe_2SiO_4 + 20Na = 8Na_4CaSi_3O_9 + Mg_2SiO_4 + 10Fe$
3.62-3.97	$10Na_2MgSi_4O_{10} + 9Fe + 12Na = 5Mg_2SiO_4 + 16Na_2Si_2O_5 + 3Fe_3Si$
3.97-4.57	$3Na_2Si_2O_5 + 3Fe + 4Na = 5Na_2SiO_3 + Fe_3Si$

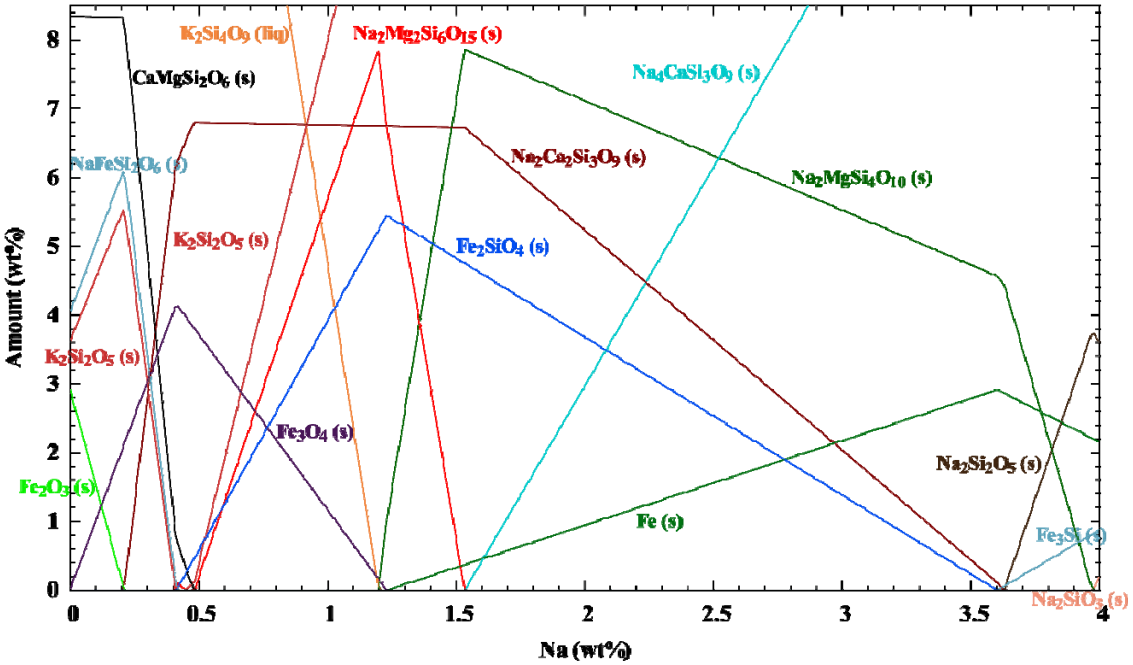

Figure 4. Exposure of the vermiculite composition up to 4 wt% sodium vapour. For simplicity, the Mg_2SiO_4(s) phase is not included, and $K_2Si_4O_9$(liq) is only partially included. See Figure 3 for these phases.

A minor formation and consumption of $Na_2Mg_2Si_6O_{15}$(s) happens in the region 0.42 - 0.48 wt% Na, see Figure 4, which has not been included in the balanced chemical reactions in Table 3.

3.3. Moler materials

In case of moler bricks, the simplified composition largely accounts for all major phases during sodium vapour exposure. The phase composition is shown in Figure 5, while the reactions are summarized in Table 4.

Table 4. Chemical reactions for the simplified moler composition when exposed to sodium vapour. The reaction number corresponds to the numbers given in Figure 5.

Reaction number	Chemical reaction
1	$16SiO_2 + Al_6Si_2O_{13} + 9Fe_2O_3 + 6Na = 6Fe_3O_4 + 6NaAlSi_3O_8$
2	$65SiO_2 + 8Al_6Si_2O_{13} + 6Fe_3O_4 + 12Na = 9Fe_2Al_4Si_5O_{18} + 12NaAlSi_3O_8$
3	$11SiO_2 + Fe_2Al_4Si_5O_{18} + 2Fe_3O_4 + 4Na = 4NaAlSi_3O_8 + 4Fe_2SiO_4$
4	$7SiO_2 + Fe_2Al_4Si_5O_{18} + 4Na = 4NaAlSi_3O_8 + 2Fe$
5	$10SiO_2 + 5Fe_2SiO_4 + 8Na = Na_8Fe_6Si_{15}O_{40} + 4Fe$
6	$5SiO_2 + Na_8Fe_6Si_{15}O_{40} + 12Na = 10Na_2Si_2O_5 + 6Fe$
7	$5SiO_2 + 3Fe + 4Na = 2Na_2Si_2O_5 + Fe_3Si$
8	$10SiO_2 + Fe_3Si + 8Na = 4Na_2Si_2O_5 + 3FeSi$
9	$5SiO_2 + FeSi + 4Na = 2Na_2Si_2O_5 + FeSi_2$
10	$2FeSi + 5NaAlSi_3O_8 + 8Na = 4Na_2Si_2O_5 + 2FeSi_2 + 5NaAlSiO_4$
11	$6FeSi_2 + 5NaAlSi_3O_8 + 8Na = 4Na_2Si_2O_5 + 2Fe_3Si_7 + 5NaAlSiO_4$
12	$3Na_2Si_2O_5 + 4Na = 5Na_2SiO_3 + Si$

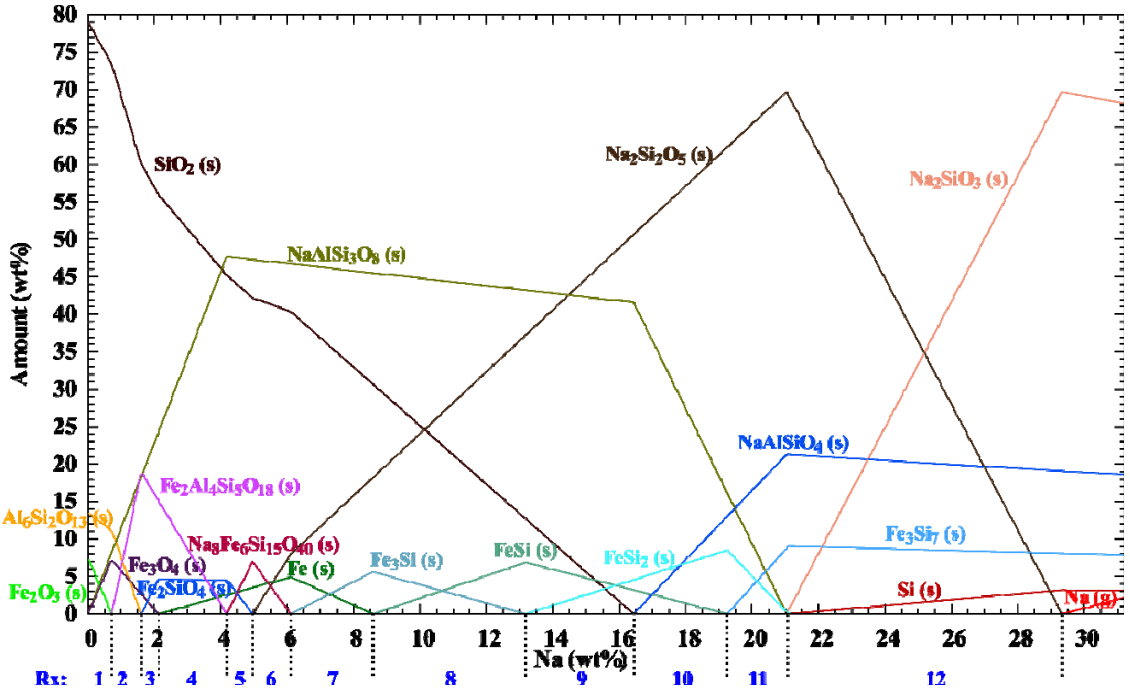

Figure 5. Exposure of the simplified moler composition to sodium vapour. No further reaction takes place after addition of approximately 29.5 wt% sodium. The blue numbers on the x-axis mark the different chemical reactions taking place.

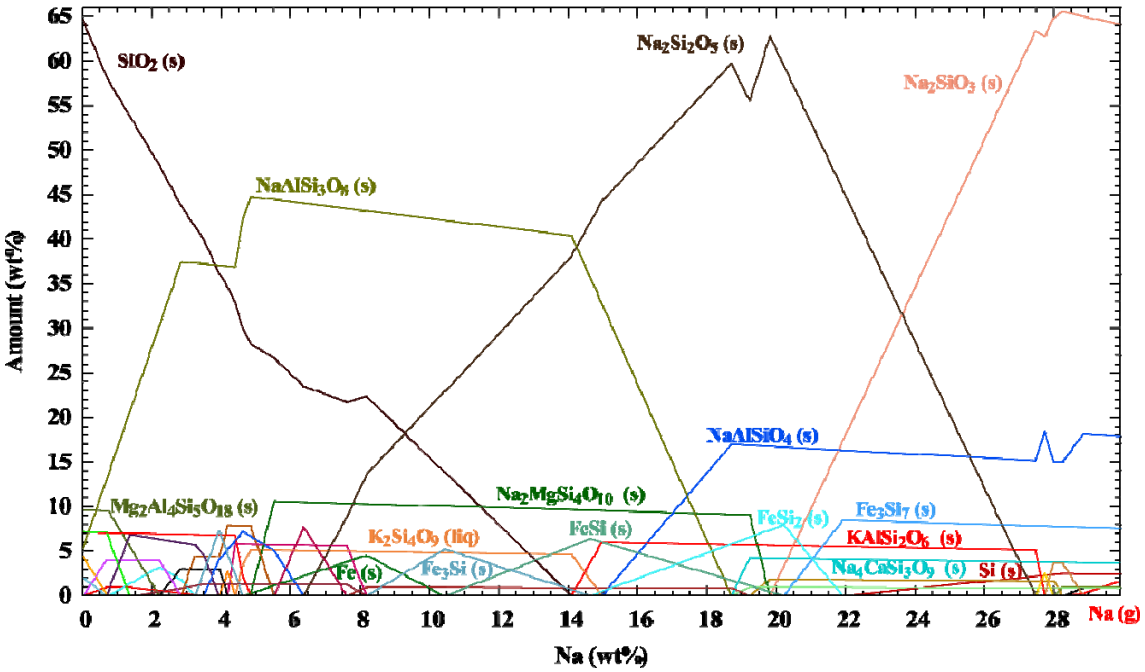

Figure 6. Exposure of the moler composition to sodium vapour. No further reaction takes place after addition of approximately 29 wt% sodium.

There are several minor phases present during the first 4 wt% of sodium vapour in case of the actual moler composition and the phase composition in this region is provided in Figure 7. Notice that the presence of the SiO_2(s) phase is not included (out of range), and the content of $NaAlSi_3O_8$(s) is only partially included. The reactions taking place during the first 4 wt% of sodium exposure of the moler composition are given in Table 5.

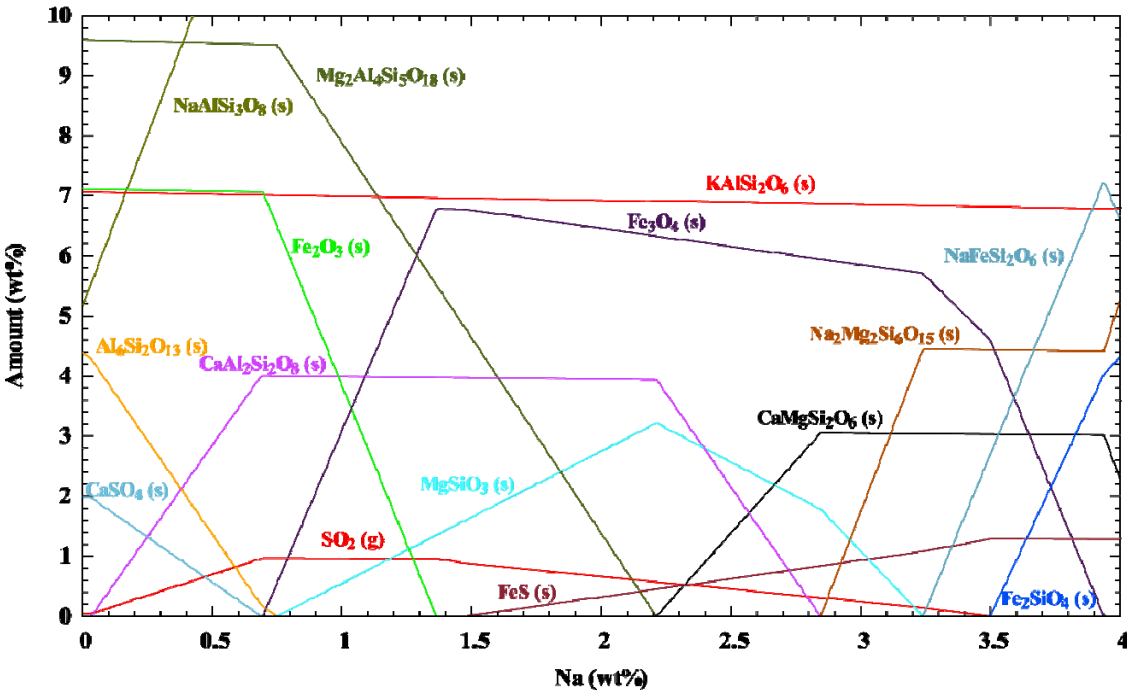

Figure 7. Exposure of the moler composition up to 4 wt% sodium vapour. For simplicity, the SiO_2(s) phase is not included, and $NaAlSi_3O_8$(s) is only partially included. See Figure 6 for these phases.

Table 5. Chemical reactions for the moler composition when exposed to up to 4 wt% sodium vapour. See Figure 7 for reference to phase compositions.

Na (wt%)	Chemical reaction
0-0.03	$2SO_3 = 2SO_2 + O_2$ $32SiO_2 + 2Al_6Si_2O_{13} + 3O_2 + 12Na = 12NaAlSi_3O_8$
0.03-0.69	$20SiO_2 + 2Al_6Si_2O_{13} + 3CaSO_4 + 6Na = 6NaAlSi_3O_8 + 3CaAl_2Si_2O_8 + 3SO_2$
0.69-0.75	$16SiO_2 + Al_6Si_2O_{13} + 9Fe_2O_3 + 6Na = 6NaAlSi_3O_8 + 6Fe_3O_4$
0.75-1.36	$9SiO_2 + Mg_2Al_4Si_5O_{18} + 6Fe_2O_3 + 4Na = 4NaAlSi_3O_8 + 4Fe_3O_4 + 2MgSiO_3$
1.36-1.47	$18SiO_2 + 2Mg_2Al_4Si_5O_{18} + 2SO_2 + 8Na = 8NaAlSi_3O_8 + 4MgSiO_3 + S_2$
1.47-2.21	$45SiO_2 + 5Mg_2Al_4Si_5O_{18} + Fe_3O_4 + 3SO_2 + 20Na = 20NaAlSi_3O_8 + 10MgSiO_3 + 3FeS$
2.21-2.85	$50SiO_2 + 10MgSiO_3 + 10CaAl_2Si_2O_8 + Fe_3O_4 + 3SO_2 + 20Na = 20NaAlSi_3O_8 + 10CaMgSi_2O_6 + 3FeS$
2.85-3.24	$40SiO_2 + 20MgSiO_3 + Fe_3O_4 + 3SO_2 + 20Na = 10Na_2Mg_2Si_6O_{15} + 3FeS$
2.88-3.50	$10SiO_2 + 2Fe_3O_4 + SO_2 + 5Na = 5NaFeSi_2O_6 + FeS$
3.50-3.94	$3SiO_2 + Fe_3O_4 + Na = NaFeSi_2O_6 + Fe_2SiO_4$
3.94-4.19	$21SiO_2 + 10NaFeSi_2O_6 + 12CaMgSi_2O_6 + 10Na = 6Na_2Mg_2Si_6O_{15} + 4Na_2Ca_3Si_6O_{16} + 5Fe_2SiO_4$

4. Discussion

The insulation materials used in aluminium reduction cells are of utmost importance to both the thermal and structural integrity of the cell. Any deformation of the insulation layer due to high temperature creep or chemical reaction would strongly reduce the thermal insulation and thereby affect the thermal balance and finally the lifetime of the cell. The most severe deterioration of the highly porous materials would be the formation of a liquid phase, which

would lead to coarsening or liquid phase sintering. The formation of liquid phases in the materials are detrimental to the microstructure of the thermal insulation bricks. On the other hand, the possible formation of a continuous viscous layer or film in the material due to formation of a liquid phase may reduce further sodium penetration and reactions with the materials.

Calcium silicate is vulnerable to sodium vapour in the sense that it is completely transformed to a new phase at only 5 wt% Na, as seen in Figure 1. In this case, the formation of a liquid phase is not predicted, and the resulting orthosilicates are stable with respect to further sodium exposure. From the Na_2O-CaO-Si_2O phase diagram however, stable liquids exist below 900 °C close to the $Na_2Ca_2Si_3O_9$(s) phase composition, meaning kinetics could favour the formation of a liquid [10].

In the case of vermiculite, the two most abundant phases in the pristine materials are Mg_2SiO_4(s) and $KAlSi_2O_6$(s), which both have high melting points [11, 12]. However, a liquid phase, $K_2Si_4O_9$(liq), is predicted even before the exposure to sodium. As seen from Figures 4 and 5, the amount of this phase is significant with 17 wt% of the total composition after only 0.5 wt% sodium. This phase is also predicted for the moler material, but not before approximately 4.5 wt% sodium. It is further worth mentioning the difference between the simplified composition (without iron) and the real composition of vermiculate. The reducing conditions provided by the sodium vapour environment favours the reduction of the less noble iron compared to the more noble silicon. In the simplified composition, the presence of iron is disregarded, hence reduction of silicon takes place.

Moler is the only material where the formation of albite, $NaAlSi_3O_8$(s), is predicted, even from the first exposure to sodium vapour (see Figures 6 and 7). It is also the most dominant product during the first 3 wt% of sodium exposure. Glassy phases close to albite have been reported to be present in reacted refractory layers of shut down cells, which normally do not crystallize [8]. The formation of albite in moler may thus be beneficial for creating a viscous barrier and hindering further sodium penetration in the highly porous material. If such a layer is not formed, further sodium exposure will form the $K_2Si_4O_9$(liq) phase, and from about 6.5 wt% the $Na_2Si_2O_5$(s) phase is predicted as the main product, reaching over 60 wt% of the material's composition after 19 wt% sodium. This compound has been reported to have a melting point below 900 °C, which could be detrimental to the structural integrity if such high sodium weight percentages are reached [10, 13].

In work performed by Tschöpe et al., a Na reaction front was found in the refractory material protecting the insulation materials [7]. The refractory was observed to contain as much as 13 wt% Na in the reaction front, and close to 20 wt% a few mm behind the reaction front, indicating the need for understanding the stability of the insulation materials when exposed to this reaction front.

5. Conclusion

The thermodynamic stability of the three most common thermal insulating materials used in aluminium reduction cells were assessed with respect to exposure to sodium vapour. A complete mineralogical transformation is predicted for calcium silicate after about 5 wt% sodium vapour. A significant amount of liquid phase is predicted to be formed at low concentrations of sodium in vermiculite materials, and may be detrimental to the structural integrity. In moler, the formation of albite is predicted during the first 3 wt% of sodium. A glassy phase with composition close to albite have previously been found in refractory linings, and this could possibly be beneficial for creating viscous barrier in the moler materials, hindering further sodium penetration.

6. Acknowledgement

Financial support from the Norwegian Research Council and Hydro, Alcoa, Elkem Carbon and Skamol, through the project CaRMa - Reactivity of Carbon and Refractory Materials used in Metal Production Technology, is gratefully acknowledged.

7. References

1 K. Grjotheim, H. Kvande, Understanding the Hall-Héroult Process for Production of Aluminium, *Aluminum-Verlag, P. O. Box 1207, D-4000 Dusseld. 1, FRG, 1986.*

2 A. Seltveit, Ildfaste materialer, *Tapir, 1992*.

3 E. Skybakmoen et al., Laboratory test methods for determining the cathode wear mechanism in aluminium cells, *Light Metals* 2007, 815–820.

4 K. Tschöpe et al., Investigation of the Cathode Wear Mechanism in a Laboratory Test Cell, *Light Metals* 2012, 1349–1354.

5 A.L. Yurkov, L.M. Aksel'rod, Properties of heat-insulating materials (a review), *Refract. Ind. Ceram.*, 46 (2005), 170–174.

6 F.B. Andersen, J. Mikkelsen, Thermal Conductivity Measurements of Cathode Insulation Materials, *Light Metals* 2000, 429-435.

7 K. Tschöpe et al., Chemical Degradation of Cathode Linings in Hall-Héroult Cells - An Autopsy Study of Three Spent Pot Linings, *Metall. Mater. Trans. B Process Metall. Mater. Process. Sci.*, 43 (2012), 290–301.

8 K. Tschöpe, J. Rutlin, T. Grande, Chemical Degradation Map for Sodium Attack in Refractory Linings, *Essent. Readings Light Met. Electrode Technol. Alum. Prod.*, 4 (2013), 978–983.

9 C.W. Bale et al., FactSage thermochemical software and databases - recent developments, *Calphad Comput. Coupling Phase Diagrams Thermochem.*, 33 (2009), 295–311.

10 Z. Zhang et al., Thermodynamic assessment of the CaO-Na2O-SiO2 slag system, *Ninth Int. Conf. Molten Slags, Fluxes Salts*, (2012).

11 B.T.C. Davis, J.L. England, The melting of forsterite up to 50 kilobars, *J. Geophys. Res.*, 69 (1964), 1113.

12 N. Brachhold, C.G. Aneziris, Synthesis of alkali aluminosilicates - Materials for alkali contaminated environments at high temperatures, *Int. J. Appl. Ceram. Technol.*, 10 (2013), 707–715.

13 F.C. Kracek, The system sodicm oxide-silica, *J. Phys. Chem.*, 34 (1930), 1583–1598.